Revised version to appear in *Monthly Notices*

Instabilities of a family of oblate stellar spheroids

J. A. Sellwood[1] and M. Valluri[1,2]
[1]*Department of Physics and Astronomy, Rutgers University, Piscataway, NJ 08855*
[2]*Department of Astronomy, Columbia University, New York, NY 10027*

Rutgers Astrophysics Preprint No 193

ABSTRACT

We have examined the stability of a sequence of oblate elliptical galaxy models having the Stäckel form suggested by Kuz'min & Kutuzov. We have employed the 2-integral DFs given by Dejonghe & de Zeeuw for which flattened non-rotating models are characterized by counter-streaming motion and are radially cool; we introduce net rotation in some models by changing the sign of the z-component of angular momentum for a fraction of the particles. We have found that all non-rotating and slowly rotating members of this sequence rounder than E7 are stable, and that even maximally rotating models rounder than E4 are stable.

In the absence of strong rotation, the most disruptive instability, and the last to be stabilized by increasing thickness, is a lopsided ($m = 1$) mode. This instability appears to be driven by counter-rotation in radially cool models. Its vigour is lessened as rotation is increased, but it remains strong even in models with net angular momentum 90% of that of a maximally rotating model before finally disappearing in maximally rotating models. Strongly rotating models are more unstable to bar-forming modes which afflict maximally rotating models with $c/a \lesssim 0.5$, but this mode is quickly stabilized by moderate fractions of counter-rotating particles. Bending instabilities appear not to be very important; they are detectable in the inner parts of the flatter models, but are less vigorous and more easily stabilized than the lop-sided or bar modes in every case. We briefly discuss the possible relevance of the lop-sided instability to the existence of many lop-sided disk galaxies.

Key words: galaxies: evolution – galaxies: kinematics and dynamics – galaxies: elliptical and lenticular – galaxies: structure – celestial mechanics: stellar dynamics – instabilities

1 INTRODUCTION

The instabilities of equilibrium stellar systems deserve attention for at least three reasons: systems known to be unstable can be excluded as possible models of galaxies, knowledge of instabilities will help us to understand how the galaxies can be altered during and after their formation into the shapes we observe today, and finally, features such as bars, spirals, boxiness and more speculatively lopsidedness, could result from instabilities.

In contrast to disk galaxies comparatively little work has yet been done on the possible instabilities of realistic pressure supported stellar systems. One of the principal reasons for this imbalance

is that it is more difficult to construct good equilibrium models of elliptical galaxies to study. The rotational support of disk galaxies, and the ready identification of the only two possible isolating integrals in razor-thin disks, has allowed many models to be constructed and their stability to be examined (see *e.g.* Sellwood 1994 for a review).

1.1 Historical survey

Antonov (1960) used a variational principle to establish a criterion for the Jeans stability of a spherical system. Subsequent work on spherical systems, nicely summarized by Binney & Tremaine (1987, §5.2), has yielded stability criteria for all modes if the distribution function (DF) is a function of energy only (isotropic models), or to radial modes only for more general DFs.

Lynden-Bell (1967) formulated the normal mode problem for inhomogeneous models, reworking Antonov's results for spherical systems and also discussing the possible stellar dynamical equivalent of the two-stream instability of plasmas. Kalnajs (1971) introduced action-angle variables and developed a matrix method (Kalnajs 1977) for searching for normal modes which has so far been applied in rather few cases.

The simple form of the gravitational potential in uniform density spheroids permits semi-analytic derivations of their normal modes (Fridman & Polyachenko 1984; Vandervoort 1991). Some of these modes have analogues in more realistic inhomogeneous models, but others are likely to be artifacts of this sharp-edged mass distribution in which all orbits have an identical set of frequencies.

May & Binney (1986) and Goodman (1988) adopt a third approach of imagining a neutral disturbance to the equilibrium and asking whether the system over-responds; this yields a stability test, but not the form or vigor of any instability, and is generally restricted to non-rotating models.

The final possible approach, which has yielded the most significant results, is to test the stability of models using N-body simulations. There are many advantages to this approach: arbitrarily complicated models can be studied without restriction on the geometrical shape or form of the DF, provided that an equilibrium model can be created. Simulations reveal all large-scale instabilities, without prior knowledge of their expected forms, and yield the non-linear evolution which could either be violently disruptive or cause a mild re-arrangement. The physical behaviour can easily be restricted, *e.g.* by imposing symmetries, in order to separate simultaneously growing modes or to obtain helpful insights into the instability mechanism. The method comes with a number of disadvantages, of course: a simulation yields only approximate frequencies and eigenfunctions of the first couple of dominant modes. Slowly growing modes may be masked by particle noise or other inadequacies making it hard to determine the marginal stability point in a sequence of models. Finally, even large-scale instabilities can be suppressed by quite modest amounts of gravity softening (*e.g.*, Sellwood 1981; 1983).

Despite its generality, this approach has been most severely restricted by the paucity of good equilibrium models to study. With the exception of the recent study by Dehnen (1996), the only non-spherical equilibria to have been examined are shell orbit models (Bishop 1987, Hunter *et al.* 1990) or numerically determined equilibria (Levison & Richstone 1987). In this paper we use an analytic DF for very simple Stäckel models. Recent progress in constructing realistic equilibria (*e.g.* Qian *et al.* 1995, Merritt & Fridman 1996) should improve this situation dramatically in the near future.

1.2 Known Instabilities

Instabilities that have been found so far fall into two broad categories: the well-known Jeans modes, in which the self-gravity of the disturbance is destabilizing, and bending modes. Bending modes, which resemble the Kelvin-Helmholtz instability in fluids or the hose instability of plasmas (Toomre 1966), are destabilized by anisotropic pressure and gravity actually provides the restoring force.

The radial orbit instability was first discussed by Antonov (1972) who argued that spherical stellar systems with a large fraction of predominantly radial orbits would be unstable to bar formation. Merritt (1987) gives an excellent review of the early work and relates the instability to Lynden-Bell's (1979) orbit alignment mechanism for bars in disks. Since this mechanism still relies on the self-gravity of the orbits, it is a Jeans-type instability. Subsequently, Saha (1992) used Kalnajs's (1977) matrix method to study the stability boundary for various non-singular models, but could find no general stability criterion. Palmer, Papaloizou & Allen (1990) showed that axisymmetric spheroidal models with a bias towards radial orbits were also unstable.

de Zeeuw *et al.* (1983) found that non-rotating, radially cold "shell orbit" models were unstable to clumping into ring ($m = 0$) modes when the mass distribution was flatter than E5.8 while Merritt & Stiavelli (1990) gave the critical boundary as E6. These modes are clearly the generalization of the well-known axisymmetric Jeans instability of stellar disks (Toomre 1964).

Lop-sided ($m = 1$) instabilities were also present in *all* the oblate models studied by Merritt & Stiavelli and in similar counter-streaming models reported by Levison, Duncan & Smith (1990, hereafter LDS). Zang & Hohl (1978) had previously discovered $m = 1$ instabilities in counter-rotating disks. Merritt & Stiavelli suggested that flattened stellar systems need a minimum amount of radial kinetic energy to be stable to this mode, a conjecture supported by Sellwood & Merritt's (1994, hereafter SM) results for disks. Robijn (1995) used the matrix method to study the unstable modes of oblate Kuz'min-Kutuzov models having little radial pressure, and again concluded that all oblate shell models are unstable to the lopsided mode. He found that adding net rotation did not affect the growth rate of the instability very much, but that it was substantially reduced by increasing the radial velocity dispersion.

Merritt & Hernquist (1991) found that strongly prolate models, again having only shell orbits with no net rotation, were unstable to bending modes. Raha *et al.* (1991) found a similar instability in a rapidly rotating triaxial bar, and SM showed that hot disks generally buckle when too thin. These modes are similar to the bending modes of stellar sheets first studied by Toomre (1966) – see Merritt & Sellwood (1994) for a more complete reference list.

LDS and SM also found that highly flattened systems with strong counter-rotation can develop two oppositely rotating bars. The latter authors conjectured that the instability which leads to each bar was the well-known bar-forming instability of disks, with the two oppositely rotating systems coupled only weakly, if at all. We question this interpretation here.

Some studies have included net rotation. LDS showed that models as flat as E6 were unstable to the formation of $m = 2$ bar modes and associated spiral modes. They identified two primary causes for the development of a bar: radial orbit instabilities which dominated in the radially hot non-rotating models and the usual bar-forming ("streaming") instability in rotating models. They found that both $m = 2$ and $m = 1$ modes were present in models with net rotation and they claimed, somewhat surprisingly, that the growth rate of the $m = 1$ mode was independent of the degree of rotation. We do not confirm this last result. Dehnen (1996) found bar instabilities in oblate "cuspy" models with net rotation.

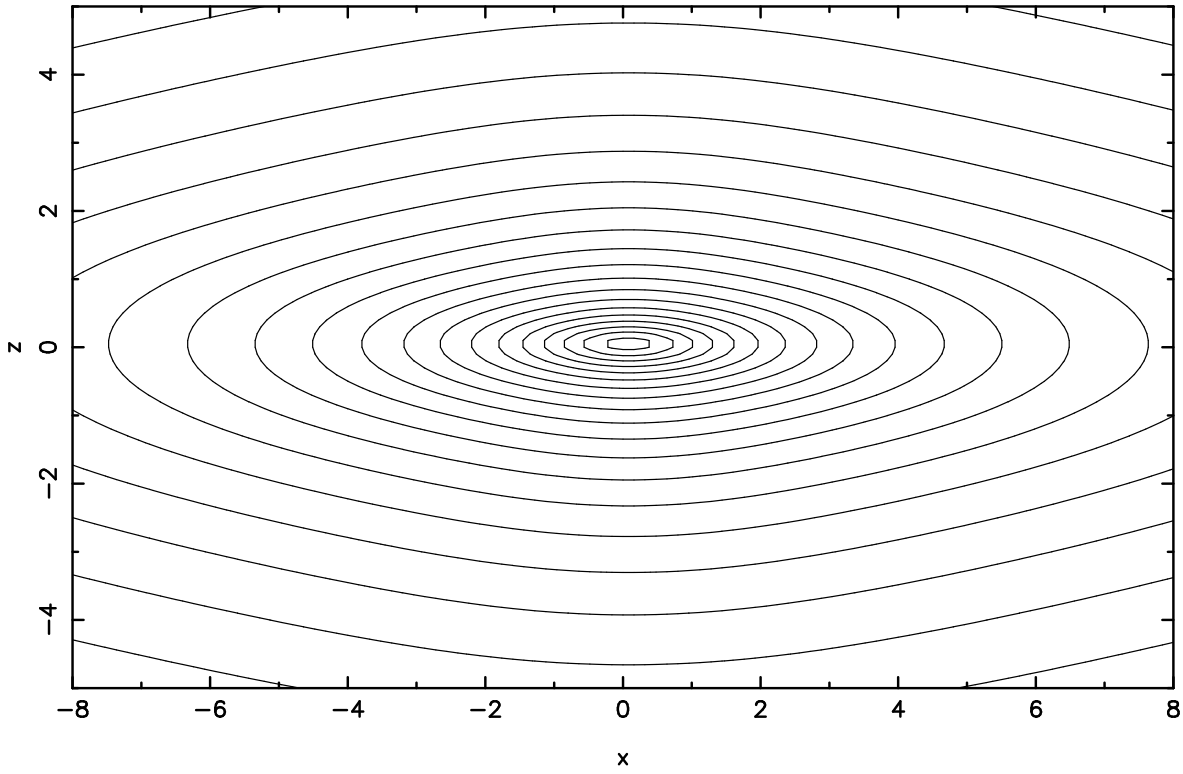

Figure 1. Contours of projected density of the $c/a = 0.2$ model, viewed from the equatorial plane.

Allen, Palmer & Papaloizou (1992) claimed that nearly spherical models that were made to rotate by flipping orbits were unstable to forming a triaxial shape, but it now appears that this result was an artifact. Similar models reported here seem quite stable.

In this paper, we present a reasonably complete study of the oblate family of Stäckel models described by Kuz'min & Kutuzov (1962) with the two-integral DFs given by Dejonghe & de Zeeuw (1988). They are still unrealistically simple in comparison with elliptical galaxies, but they are an improvement over many of the studies reported above because they are neither spherical, nor uniform density, nor are they shell orbit models.

2 TECHNIQUE

2.1 The Kuz'min-Kutuzov Model

Kuz'min & Kutuzov (1962) describe a set of inhomogenous axisymmetric mass models of Stäckel form. Dejonghe & de Zeeuw (1988) derived several DFs for these models, but we have restricted our study to the stability of their two-integral oblate models, which for brevity we refer to as the KKDZ models.

In cylindrical polar coordinates, the models have the potential

$$\Phi(R,z) = \frac{GM}{(R^2+z^2+a^2+c^2+2\sqrt{a^2c^2+c^2R^2+a^2z^2})^{1/2}}, \tag{1}$$

and density

$$\rho(R,z) = \frac{Mc^2}{4\pi}\frac{(a^2+c^2)R^2+2a^2z^2+2a^2c^2+a^4+3a^2\sqrt{a^2c^2+c^2R^2+a^2z^2}}{(a^2c^2+c^2R^2+a^2z^2)^{3/2}(R^2+z^2+a^2+2\sqrt{a^2c^2+c^2R^2+a^2z^2})^{3/2}}, \tag{2}$$

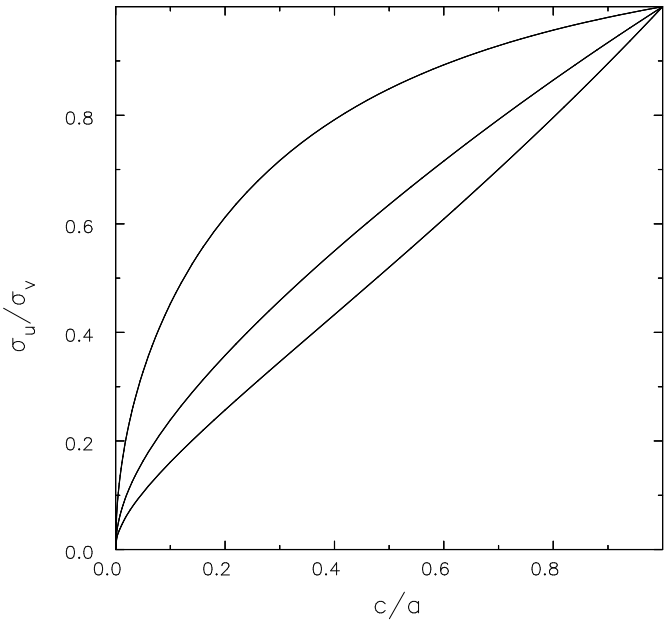

Figure 2. The axis ratio of the velocity spheroid in the equatorial plane as a function of flattening. From top to bottom, the three curves show values at $R = 0.5, 1.3$ & 3.0 respectively.

where M is the total mass. Models with $c < a$ are oblate and models with $c > a$ are prolate. The family includes the spherical isochrone (Hénon 1959) when $a = c$, and the Kuz'min-Toomre disk (Kuz'min 1956, Toomre 1963 model 1) when $c = 0$.

The surfaces of constant density are flattened spheroids and models become more spherical with increasing radius (Dejonghe & de Zeeuw 1988, Figure 5); the density falls off as r^{-4}. The fiducial axis ratio c/a is typically slightly smaller than the central axis ratio in the oblate case and slightly greater than the central axis ratio in the prolate case. The true axis ratio approaches the limiting value, ξ_∞, given by

$$\xi_\infty^4 = \frac{2c^3}{a(a^2+c^2)}. \tag{3}$$

As all our models are truncated at $R = 5(a + c)$, the outer axis ratio is slightly less than the asymptotic value.

The *projected* density profile of the $c/a = 0.2$ model, viewed from the symmetry plane to show maximum flattening, is shown in Figure 1. We will show in §3 that this approximately E7 galaxy model is the flattest stable member of the KKDZ family, except for maximally rotating models.

Dejonghe & de Zeeuw applied inversion methods to derive a two-integral DF for these spheroids. For a given c/a, they find

$$F(E, J_z^2) = \frac{1}{2^{3/2}\pi^3}\frac{c^2}{a}E^{5/2}\times \\ \left[\sum_{\epsilon=-1,1}\int_0^1 \frac{1-t^2}{(1-2aEt\sqrt{1-t^2}+\epsilon t\sqrt{z})^5}\left[(3+4x_\epsilon-x_\epsilon^2)(1-x_\epsilon)(1-t^2)+12t^2\right]dt\right], \tag{4a}$$

where,

$$x_\epsilon = \frac{2aEt\sqrt{1-t^2}}{1+\epsilon t\sqrt{z}}, \qquad z = 2AEJ_z^2, \qquad A = \frac{a^2-c^2}{a^2}. \tag{4b}$$

(Two typographical errors in the original published expression have been corrected here.) This DF is nowhere negative for $c < a$ and is therefore physical for all oblate models.

Since these are two-integral models, the radial, σ_u, and vertical, σ_w, velocity dispersions are always equal, and flatter models have less radial pressure. Flat models with no net rotation are characterized by equal and opposite streams of particles; Figure 2 shows the variation of σ_u/σ_v with c/a, with σ_v defined as the rms velocity of this counter-streaming distribution at three different radii in the equatorial plane: $(R, z) = (0.5, 0)$, (1.3,0), where the streaming velocity dispersion is close to maximum, and (3,0). The anisotropy of the velocity distribution increases with radius for flat models but becomes isotropic everywhere for the sphere.

To make the models finite, we eliminate all particles having an energy greater than the gravitational potential in the mid-plane at $R = 5(a + c)$. We ignore the small imbalance this truncation introduces since the initial virial ratios $T/|W|$ are within a few percent of the equilibrium value of 0.5.

We adopt units where $G = M = a + c = 1$. The central potential $\Phi(0, 0) = 1$ in these units.

2.2 Quiet Start

We generate particles by selecting pairs of (E, J_z) values having the density of this DF using a technique similar to that described by Sellwood & Athanassoula (1986). It ensures that the pairs of integrals of our selected particles have the smoothest possible distribution for a discrete sample drawn from the desired 2-integral DF. Having selected the integrals deterministically, we choose the initial orbital phases randomly, which we justify by appealing to past experience with disks. Sellwood (1983) and Earn & Sellwood (1995) found that growth rates of non-axisymmetric instabilities were not much affected by how carefully the angles were chosen.[1] For each pair of integrals, we position one or more particles (up to 5) by choosing (R, z) pairs from the allowed region of the meridional plane (where the probability density is uniform) and an azimuthal phase for each. The values of E and J_z almost determine the velocity components at the chosen position – all that remains is to direct the component in the meridional plane with the help of one further random number.

In order to determine the unstable modes of the model, in addition to requiring that the particles are the best possible sample from the DF, we also require a distribution that is both at rest and perfectly centered on our coordinate origin and that the seed amplitude of all unstable modes is much lower than is possible with a random distribution of particles. To achieve this, we use each coordinate set generated as described in the previous paragraph to place two particles in mirror symmetric positions about the $z = 0$ plane with oppositely directed vertical velocity components and then place six such pairs of particles equally in azimuth. This procedure automatically centers the model and eliminates all three linear momentum components; we can also eliminate net angular momentum, if desired, by reversing the azimuthal components of half these particles. Imposing six-fold rotational symmetry reduces the seed amplitude of all low-order non-axisymmetric modes, which include all the most important instabilities.[2]

[1] In this 3-D Stäckel model, however, we might have obtained more precise results had we enforced a uniform density in the third integral.

[2] A study of axisymmetric oscillations, on the other hand, would require a different strategy – one designed to suppress noise in the radial density profile.

2.3 Rotation

The equilibrium of an axisymmetric stellar system is unaffected when an arbitrary fraction of the stars have their angular momentum about the symmetry axis reversed. We are therefore able to introduce azimuthal streaming motion by using Lynden-Bell's (1962) daemon to reverse the sign of J_z for a fixed fraction of particles. Following LDS, we define the parameter

$$\eta = \frac{\sum J_{z_i}}{\sum |J_{z_i}|}. \tag{5}$$

This parameter varies from zero for models with no net rotation to unity when all particles orbit in the same sense. When $\eta = 0.5$, the system has half the maximum possible angular momentum: 75% of the particles are orbiting in the direct sense and 25% are retrograde.

It should be noted that an orbit flipping rule which takes no account of the magnitude of J_z will introduce a discontinuity in the DF across $J_z = 0$. Since Kalnajs (1977) warned that such a discontinuity will aggravate the bar mode, it is better to taper the flipping rule so that no signs are changed when $|J_z|$ is small, up to the full desired fraction for $|J_z| > 0.2\sqrt{GMa}$ say. We find that tapering the discontinuity in this way reduces the net angular momentum of a maximally streaming model by a percent or so, but decreases the growth rate of bar mode by more than a factor of two.

2.4 Numerical details

We use a 3-D polar grid-based N-body code which is a straightforward generalization of Sellwood's (1981) 2-D code, with the central hole eliminated. The grid planes are equally spaced in z and we solve for the gravitational field of the mass distribution using FFTs in the vertical and azimuthal directions and by direct convolution in the radial direction. The method closely resembles that described by Pfenniger & Friedli (1993) except that we solve separately for the three components of the gravitational force field and for the potential, which eliminates the need for numerical differences of the potential to find the force components. We adopt the standard (Plummer sphere) softening prescription to prevent strong forces at short range; the fixed softening length is comparable to the vertical spacing of the grid planes but is smaller than the horizontal mesh cell dimensions at large distances from the symmetry axis.

We use linear interpolation between the grid points both for mass assignment and to determine accelerations. We advance the motion of each particle using simple time-centered leap-frog in Cartesian coordinates.

The grid in most of our simulations has 80 nodes in azimuth, 65 in the radial direction and 225 vertically. We vary the z-spacing of the grid planes in order to ensure the best possible spatial resolution while keeping the whole model within the grid boundaries: typically $c/10 < \delta z \sim c/5$ so that the spacing (and softening length) is small compared with any scale on which the density varies. We use 1.2×10^5 particles and a time step of $0.05\sqrt{(a+c)^3/GM}$. Test runs with ten times the number of particles produced essentially identical results. Results did vary, however, with changes to the softening length and vertical grid spacing. Results using finer grids were not significantly different, but we found that grids coarser than our standard size generally led to lower growth rates.

We evaluate and save coefficients of a low-order spherical Bessel function expansion of the particle distribution at frequent intervals throughout the run. We then use the mode fitting procedure described by Sellwood & Athanassoula (1986) to estimate eigenfrequencies of the most unstable modes during the period of exponential growth.

Some models possessed several different instabilities which grow at different linear rates and saturate at different times. Linear modes are decoupled from each other at small amplitude, but all are affected as soon as one begins to saturate. The most rapidly growing mode is easily measured but it may saturate before other instabilities have grown sufficiently to yield reliable eigenfrequencies. We can, however, study the modes individually by re-running the same initial conditions with the disturbance forces restricted to a single non-axisymmetric Fourier harmonic. The Jeans or bending mode of that single harmonic develops separately in each run, prolonging the linear growth period for the milder instabilities and allowing us to measure the growth rates of more slowly growing instabilities. It is also possible to impose reflection symmetry about the mid-plane to suppress the bending mode when both Jeans and bending instabilities of the same azimuthal symmetry are present. The highly flattened models were unstable to axisymmetric Jeans modes, which can be suppressed by setting the axisymmetric field components to the analytic expressions.

3 RESULTS

In this section we summarize the results of our study of the KKDZ models. Our chief objectives are to establish the stability boundaries in non-rotating models, to determine the influence of rotation, and to search for possible instabilities in models rounder than E6. The eigenfrequencies, in units of $\sqrt{GM/(a+c)^3}$, of the non-axisymmetric instabilities in all the models we have run are summarized in Tables 1-3.

3.1 Axisymmetric modes

The two-integral DF naturally implies that $\sigma_u = \sigma_w$; therefore thinner models are also radially cooler. Those with axis ratios $c/a < 0.09$ (corresponding to an asymptotic axis ratio of 0.2) were violently unstable to the axisymmetric Jeans instability. We have not estimated growth rates for these modes, since they start from high amplitude and saturate quickly. Our stability boundary, $c/a = 0.1$ or E7.7, is flatter than the E5.8 given by de Zeeuw *et al.* (1983) and E6 suggested by Merritt & Stiavelli (1990) for shell orbit models. This difference is hardly surprising since radial pressure, which contributes to stability (Toomre 1964), rises as our models become less flat. These instabilities are unaffected by rotation.

3.2 Lopsided Modes ($m = 1$)

As in the case of previous studies of models with strong counter-rotation (*e.g.*, Merritt & Stiavelli 1990; LDS; SM), we found a non-rotating lop-sided instability in the flatter models. Rounder models with $c/a \gtrsim 0.2$ required special care because despite having cancelled net momentum at the start, a lateral motion of the model causes spurious growth in $m = 1$ coefficients determined from a fixed center. We could eliminate an apparent slow instability by re-centering the distribution of particles every 20 steps.

Figure 3(a) shows that the growth rate, γ, of this mode decreases with increasing c/a. N-body methods are not well suited to pinpointing a stability boundary with accuracy, but both the trend from the growth rates and the fact that we could not detect an instability in models with $c/a \geq 0.2$ strongly suggests a stability boundary of the lop-sided mode lies at a fiducial axis-ratio of $c/a \simeq 0.2$, which corresponds to an E7 galaxy (Figure 1).

Merritt & Stiavelli and Robijn (1995) had found that even slightly oblate models are lop-sided unstable, but their models had little or no radial pressure while the radial pressure in our two-integral models rises as they become rounder. Our result supports Robijn's finding that an increase in radial pressure has a considerable stabilizing effect.

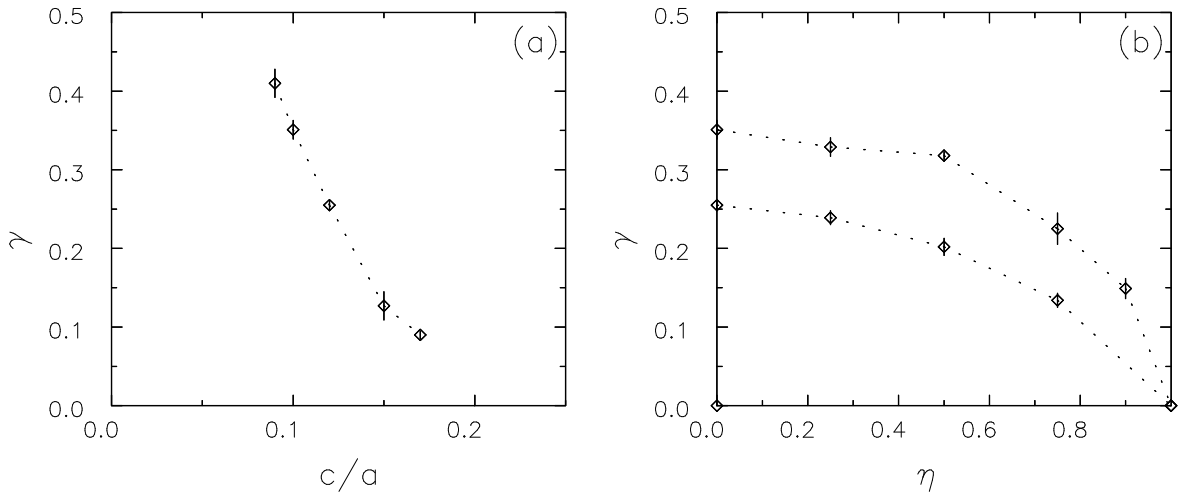

Figure 3. Growth rates of lop-sided modes in (a) non-rotating models and (b) two sequences of rotating models with $c/a = 0.1$ (upper) and $c/a = 0.12$. We have joined the measured values with dotted lines merely to indicate sequences.

The lopsided instability persists in slowly rotating models, and disappears only for maximally rotating cases. The mode has a non-zero pattern speed and resembles a one-armed spiral in models with intermediate values of η. Figure 3(b) shows the dependence of the growth rate on the degree of rotation for two sequences of models with different axis ratios. In both cases we find that while γ decreases as net rotation is increased, the instability remains quite strong when η is even as large as 0.9 and disappears only when all the particles orbit in the same sense. Note that, LDS reported no dependence on the degree of rotation; the reason for this difference is unclear.

Figure 4 shows the axis ratio of the velocity ellipsoid before and after the instability saturates. As in the case of the models studied by Merritt & Stiavelli this figure shows that the primary effect of the non-linear evolution of the lopsided mode is an increase in the radial velocity dispersion at the cost of the rms velocity of the counter-streaming motion. Thus while the initial model was supported largely by azimuthal motions the instability leads to one supported more by radial pressure.

We do not have a convincing mechanism for the lop-sided mode, though its disappearance in maximally rotating models clearly indicates that counter-rotation is responsible. Comparison of our results with those of Merritt & Stiavelli and Robijn shows also that increasing radial pressure, more than decreasing oblateness, stabilizes the mode. Some analytic work has been done for counter-rotation in disks: Palmer (1994, §12.5) provides a mathematical description in the WKBJ approximation which, however, does not offer much physical insight. Araki (1987) and Lovelace, Jore & Haynes (1996) argue that it could perhaps be the first known stellar dynamical analogue of the two-stream instability of plasmas.

3.3 Counter-rotating bars

Unlike LDS and SM, our non-rotating models generally did not form pairs of counter-rotating bars. Some of our axisymmetrically unstable models developed counter-rotating bar-like features after the ring instability saturated, but when axisymmetric forces were held rigid and disturbance forces confined to $m = 2$, the model exhibited an $m = 2$ bending mode (§3.5) only. There were no hints of linearly growing, bi-symmetric, Jeans-type disturbances – the amplitudes of $m = 2$ *density* variations merely rose incoherently as the quiet start slowly disrupted.

Table 1. Growth rates of lop-sided instabilities determined from the models

c/a	η	growth rate	pattern speed
0.09	0.00	0.410 ± 0.018	
0.10	0.00	0.351 ± 0.012	
0.12	0.00	0.255 ± 0.006	
0.15	0.00	0.127 ± 0.018	
0.17	0.00	0.090 ± 0.005	
0.20	0.00	undetectable	
0.10	0.00	0.351 ± 0.012	
0.10	0.25	0.329 ± 0.012	0.115 ± 0.003
0.10	0.50	0.318 ± 0.005	0.231 ± 0.006
0.10	0.75	0.225 ± 0.020	0.297 ± 0.011
0.10	0.90	0.149 ± 0.013	0.353 ± 0.016
0.10	1.00	undetectable	
0.12	0.00	0.255 ± 0.006	
0.12	0.25	0.239 ± 0.009	0.088 ± 0.002
0.12	0.50	0.202 ± 0.011	0.162 ± 0.009
0.12	0.75	0.134 ± 0.009	0.214 ± 0.009
0.12	1.00	undetectable	

We have traced the source of this initially puzzling discrepancy to a difference in initial seed amplitude of the $m = 2$ noise in the particle distribution at the start. LDS did not adopt any special precautions to suppress particle noise, and the procedure adopted by SM imposed bi-symmetry, thereby *raising* the initial amplitude of the $m = 2$ Fourier component above that expected from a random distribution of particles. By contrast, the particle distribution in our present simulations was made six-fold symmetric (§2.2), thus ensuring that $m = 2$ components of the noise were very weak at the start.

We have verified in a number of ways that particle noise is the principal source of the discrepancy. The most direct was to test these models with the initial bi-symmetric arrangement used by SM. With this start, and with only $m = 2$ terms contributing to the disturbance forces, a pair of large-amplitude, counter-rotating bars developed in a model with $c/a = 0.8$ and weaker bars could also be detected in another model with $c/a = 0.1$.

Our suspicions having been aroused, we used Sellwood's (1981) 2-D polar grid code for a quick and inexpensive study of similar disks. We examined the stability of Kuz'min-Toomre disks with DFs given by Kalnajs (1976) – the same family as used by Athanassoula & Sellwood (1986) and as thickened disks by SM. We first studied a half-mass, cool KT disk with the counter-rotating population replaced by rigid mass and found it to be quite stable when a quiet start was employed, but a bar formed in a noisy start model. The bar appeared to form as a result of non-linear trapping caused by swing-amplified spiral disturbances (*e.g.* Toomre 1981) seeded by the random particle distribution. Even though noise seeds all Fourier components equally, and the swing amplifier is

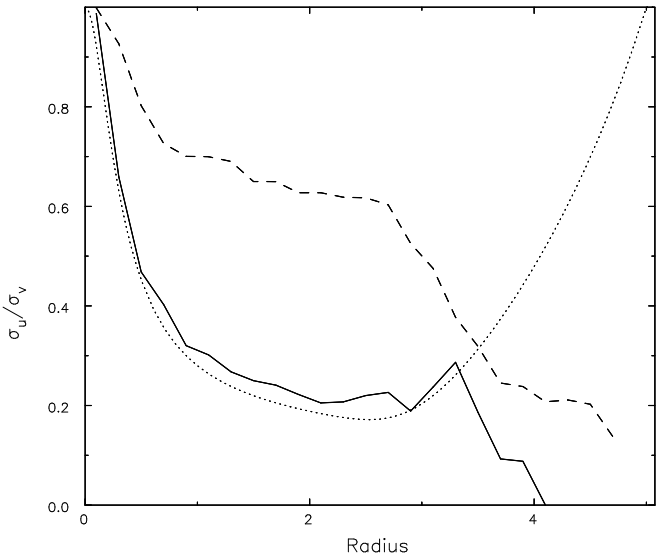

Figure 4. The axis ratio of the velocity ellipsoid before (full-drawn) and after (dashed) the instability saturates. The dotted curve shows the expected value of this ratio in the mid-plane of this truncated model at the start; the empirical values differ from the expected curve in the outer region because the particle density is so low.

effective for several low-order symmetries, large-amplitude bars develop because trapping is much easier for $m = 2$ due to the slow variation of $\Omega - \kappa/2$ (see Binney & Tremaine 1987 §6.2.1.a).

When the rigid mass was replaced by a live population of counter-rotating particles, both populations formed bars in this way, usually of similar but not exactly equal strength and not always at the same time. It is curious that bars formed quite readily in a cool ($Q \sim 1$) disk, but not in a cold disk; if all the orbits were precisely circular, and the axisymmetric part of the force was held rigid, the spirals seeded by the noise were very tightly wrapped and appeared unable to transport enough angular momentum to trap particles into a bar – at least until random motion had built up significantly. Note that SM also reported that no counter-rotating bars developed in their cold disk.

Thus the conjectures by LDS and by SM that the counter-rotating bar pairs they found were formed through linear instabilities seem unlikely to be correct; the bars in fact result from non-linear orbit trapping in finite-amplitude spiral disturbances. Paradoxically, modest random motion aggravates this finite-amplitude instability, although very hot systems are again stable. A finite-amplitude instability also makes it easier to understand SM's finding that imposing reflection symmetry, thereby suppressing the $m = 2$ bending mode, considerably delayed the formation of the counter-rotating bars.

3.4 Bar and Spiral Modes

A bar instability, absent in quiet start non-rotating models, appears as rotation is increased. Table 2 gives two sets of frequencies for the bar modes which are determined from models both with and without a discontinuity in the DF at $J_z = 0$. Smoothing the discontinuity, as described in §2.3, leads to the values of η shown, while the values of η for the models with the discontinuity are 1.0 and 0.75 precisely; evidently the discontinuity has a huge effect on the growth rates of bars (see Kalnajs 1977).

Figure 5 shows our estimated growth rates for the $m = 2$ mode from the smoothed models as a function of axis-ratio for two values of the rotation parameter η. The growth rate drops rapidly both as the models become rounder and as net rotation is reduced. We could not detect any

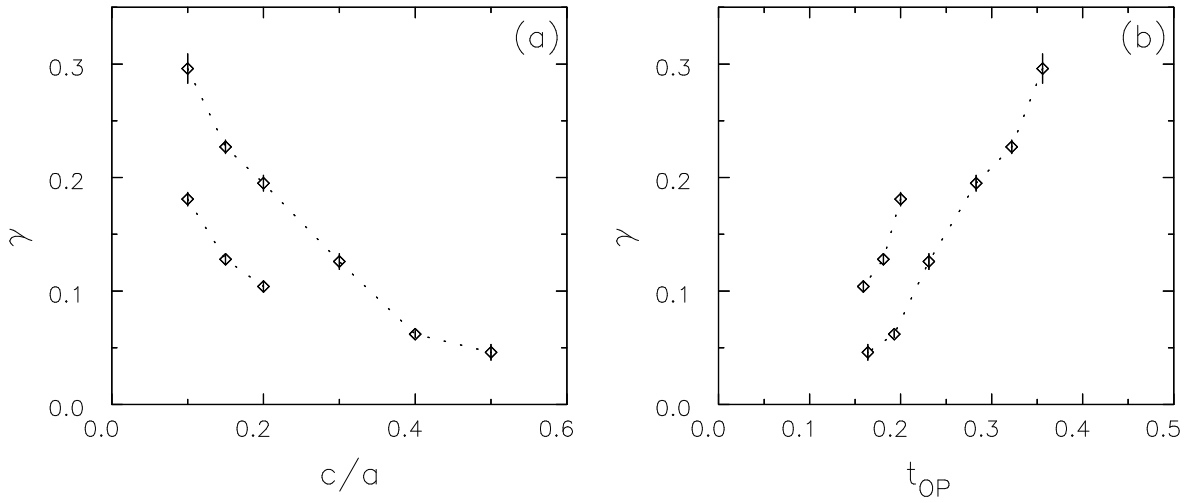

Figure 5. Growth rates of bar modes in rotating models with a smoothed DF plotted as function of (a) axis ratio and (b) the Ostriker-Peebles t parameter. The longer sequence is for $\eta \sim 1$ while $\eta \sim 0.75$ for the shorter sequence.

Table 2. Growth rates of bar instabilities determined from the models

			smoothed DF		discontinuous DF	
c/a	η	$t_{\rm OP}$	growth rate	pattern speed	growth rate	pattern speed
0.10	0.992	0.356	0.296 ± 0.013	1.002 ± 0.020	0.695 ± 0.005	1.471 ± 0.029
0.15	0.990	0.322	0.227 ± 0.006	0.830 ± 0.008	0.431 ± 0.011	1.261 ± 0.017
0.2	0.989	0.283	0.195 ± 0.007	0.769 ± 0.006	0.364 ± 0.023	1.111 ± 0.016
0.3	0.984	0.231	0.126 ± 0.007	0.671 ± 0.004	0.196 ± 0.004	0.915 ± 0.001
0.4	0.979	0.193	0.062 ± 0.003	0.623 ± 0.002	0.139 ± 0.001	0.838 ± 0.003
0.5	0.974	0.164	0.046 ± 0.007	0.528 ± 0.014	0.092 ± 0.006	0.756 ± 0.005
0.10	0.744	0.200	0.181 ± 0.006	0.880 ± 0.004	0.431 ± 0.011	1.254 ± 0.014
0.15	0.743	0.181	0.128 ± 0.004	0.692 ± 0.004	0.199 ± 0.009	1.052 ± 0.017
0.2	0.742	0.159	0.104 ± 0.005	0.635 ± 0.005	0.119 ± 0.006	0.833 ± 0.015

convincing instabilities in models with rotation parameter $\eta \lesssim 0.5$ nor in any a maximally rotating model rounder than $c/a = 0.5$. There was just a hint of a coherent rotating wave in the maximally rotating model with $c/a = 0.6$, but we could not determine a credible growth rate and we therefore suspect this model is stable, but only barely so.

The Ostriker-Peebles (1973) stability parameter, $t_{\rm OP}$, also given in Table 2 for the smoothed models, appears to correlate well with our estimated growth rates. The trends in Figure 5(b) suggest that models with $0.1 < t_{\rm OP} < 0.15$ would have zero growth rates – close to the suggested critical value of $t_{\rm OP} \sim 0.14$. It is no surprise that this stability indicator works for our models, as it has been found to be serviceable for all models with approximately harmonic cores.

The instability has the classic bi-symmetric spiral shape so often seen in rotationally supported disks and is especially strong in flatter models. While the swing-amplified feed-back loop described by Toomre (1981) seems to account for many aspects of bar instabilities in thin disks, the picture

of a feed-back loop using thin-disk density waves would have to be stretched unrealistically in the rounder members of our sequence, which are also radially much hotter. Sellwood's (1981; 1983) finding that surprisingly little gravity softening could inhibit bar instabilities in a zero-thickness disk suggests that thin-disk density waves are quickly weakened by increasing thickness, but his result also contrasts with the persistence of bar-forming instabilities to $c/a = 0.5$ in the present models. Clearly, a thick, hot spheroid has different stability properties from a softened thin disk. Thus it seems possible the bar-forming instability in the thicker models may be more closely related to the Riemann-type deformations of Maclaurin spheroids (*e.g.*, see Binney & Tremaine 1987, §5.3.5) while disk-like wave mechanics may offer a better description of the mode in thinner systems.

The stability of our nearly spherical models contrasts with the findings of Allen, Palmer & Papaloizou (1992) who reported $m = 2$ instabilities in nearly spherical models with even small amounts of rotation. To ensure that our different result was not due to the different models used, we checked the stability of their models, even using the same file of initial particle coordinates (kindly supplied by A. J. Allen), but found their model to be completely stable. The discrepancy was eventually traced to an artifact in their N-body code caused by sub-division of time steps without recalculating the potential; they now concur that their rotating nearly round models were stable.

3.5 Bending Modes

The only bending instability we found was a mild $m = 2$ "saddle" mode in highly flattened, slowly rotating, models. This instability could be reliably detected only in quite flattened models with little net rotation where it was always dominated by the lop-sided mode. It is clearly much less vigorous that the bar mode in more rapidly rotating models, but we cannot confirm its presence in this regime.

Figure 6 shows the growth rates for various values c/a for non- and slowly rotating models, indicating that those flatter than $c/a = 0.17$ were unstable. In order to measure meaningful linear growth rates for this mode, we have to suppress the lop-sided mode, by eliminating $m = 1$ disturbance forces, and axisymmetric disturbances in models with $c/a < 0.1$. At a fixed axis ratio, the growth rate is reduced slightly by small net rotation, but the bar instability prevents us from tracing the trend with increasing net rotation any further. Since this bending instability is driven by counter-rotation, it presumably disappears for maximally rotating models. We found that the bends developed in the inner regions only where the models are flatter (see Figure 1) and the radial extent of the mode decreased with increasing thickness.

The mechanism for bending modes discussed by Merritt & Sellwood (1994) accounts pretty well for this instability in the present models. Their instability criterion requires that frequency of small-amplitude vertical oscillations in the mid-plane exceed twice (for $m = 2$) the circular frequency. The instability criterion was clearly satisfied in the radial ranges where the instability was seen and is not satisfied anywhere when $c/a \gtrsim 0.2$. However, their criterion marginally predicts instability when $c/a = 0.17$ whereas none was detected; the slight failure here is probably due to the fact that the vertical oscillation period of nearly every particle exceeds that in the exact mid-plane, and therefore too few particles could co-operate to sustain an instability in this case.

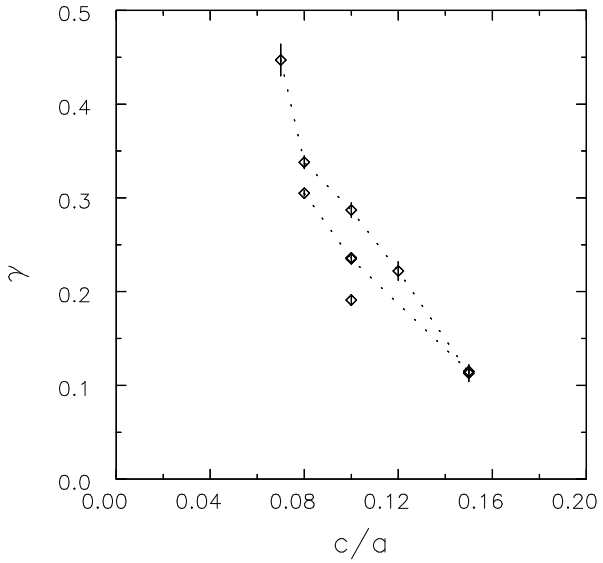

Figure 6. Growth rates of saddle modes plotted as function of axis ratio. The two sequences are non-rotating ($\eta = 0$ upper) and slowly rotating ($\eta = 0.25$).

Table 3. Growth rates of $m = 2$ bending instabilities determined from the models

c/a	η	growth rate	pattern speed
0.07	0.00	0.447 ± 0.017	
0.08	0.00	0.338 ± 0.007	
0.10	0.00	0.287 ± 0.008	
0.12	0.00	0.222 ± 0.010	
0.15	0.00	0.113 ± 0.009	
0.17	0.00	undetectable	
0.10	0.15	0.236 ± 0.001	0.050 ± 0.002
0.08	0.25	0.305 ± 0.003	0.106 ± 0.003
0.10	0.25	0.235 ± 0.005	0.088 ± 0.002
0.15	0.25	0.115 ± 0.001	0.055 ± 0.004
0.10	0.50	0.191 ± 0.006	0.169 ± 0.003

4 LOP-SIDED GALAXIES

Many galaxies have some degree of asymmetry (*e.g.* Richter & Sancisi 1994; Rix & Zaritsky 1995): the most striking nearby cases include the LMC and M101. The origin of these asymmetries is still unclear – not one of several possible ideas has seemed sufficiently promising to have been worked out in detail. The asymmetries could be residuals of (late) galaxy formation, or have been caused by recent interactions, or they could be long-lived $m = 1$ density waves (Baldwin, Lynden-Bell & Sancisi 1980; Earn 1993), or a weakly damped mode (Weinberg 1994), or finally they could result from lop-sided instabilities.

In principle, a dynamical instability would be the most attractive explanation, since it would not require an external agent to excite it. Unfortunately neither of the two known types of lop-sided instability seems promising; as we have again shown, strong counter-rotation provokes a lop-sided

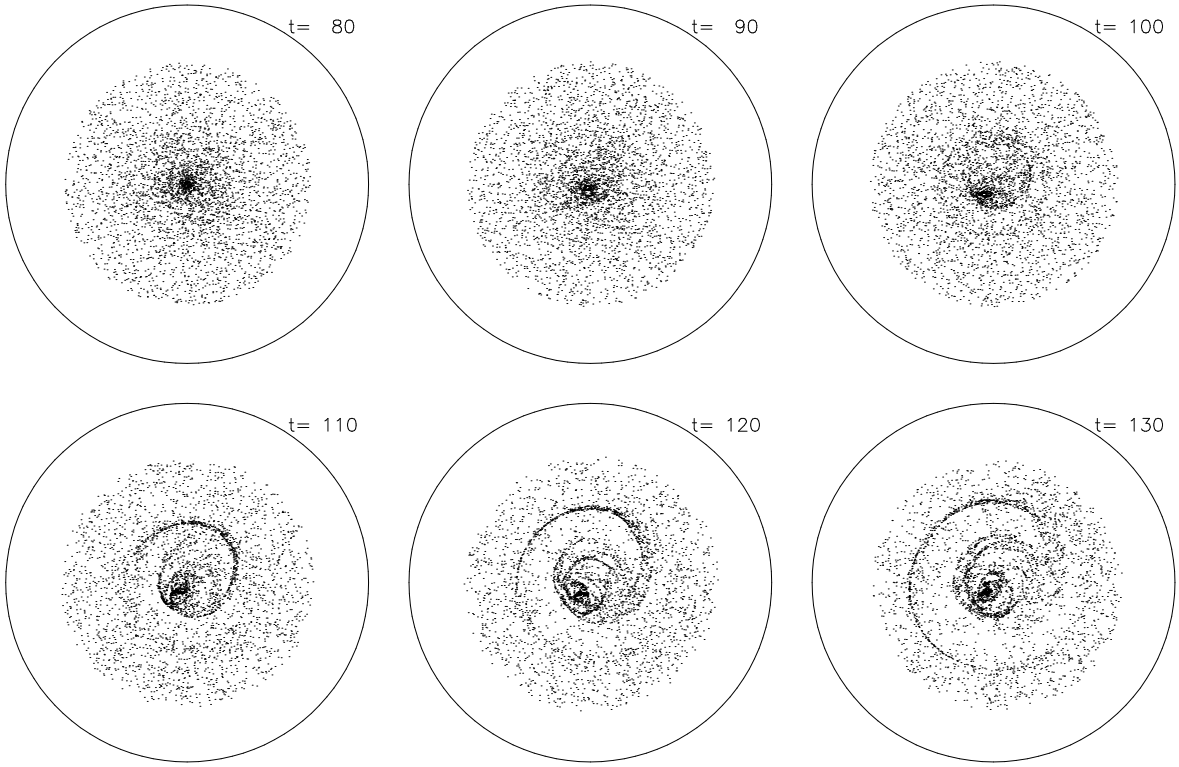

Figure 7. The evolution of a disk of test particles embedded in a "dark halo". A lop-sided instability in the halo begins to saturate at about time 100 and remains strong for some time.

instability, but large fractions of counter-streaming stars are believed to be rare (*e.g.*, Kuijken, Fisher & Merrifield 1996). The other lop-sided instability (Zang 1976; Sellwood 1985) requires a massive disk surrounding a dense nucleus in which the rotation curve is flat or slightly falling, but this does not seems promising either since many lop-sided galaxies have rising rotation curves.

It occurs to us, however, that the absence of counter-rotation in the visible matter does not preclude counter-rotation in the dark matter. A strongly flattened dark halo supported by counter-rotation could be lopsided unstable. Indeed, recent studies of the polar-ring galaxy NCG 4650A (Sackett & Sparke 1990, Sackett *et al.* 1994) have concluded that the dark halo of this system could be as flat as E6-E7 and Olling's (1996) study of flaring of the HI layer in NGC 4244 also suggests a flattened halo. On the face of it, we do not think it likely that flattened dark halos would be supported by counter-streaming, but the hypothesis could not be refuted by direct observation. In order to study the consequences for a low mass disk that might happen to reside in a counter-rotating halo, we have introduced a disk of test particles into one of our lop-sided unstable models.

Figure 7 shows part of the evolution of a disk of test particles lying in the equatorial plane of the non-rotating $c/a = 0.15$ (approximately E7) KKDZ model. The test particles were given the appropriate orbital velocity (in the anti-clockwise direction) to balance the central attraction from the KKDZ model particles, which are not plotted. The initial rotation curve of this disk rises to a maximum at $R \simeq 1.0(a+c)$ and then declines slowly to $\sim 85\%$ of the maximum rotation speed at the outer edge at $R = 4(a+c)$. The response of this disk to the non-rotating lop-sided instability first produces a lateral shift in the inner third of the disk and then a one-arm leading spiral with an asymmetric density distribution in its interior.

The spiral arm, which is caused by a growing forcing amplitude, dissolves at later times as the whole particle distribution becomes increasingly disturbed. We have chosen to determine the velocity field from the particles at a moment when the lop-sidedness is strong but before the particle

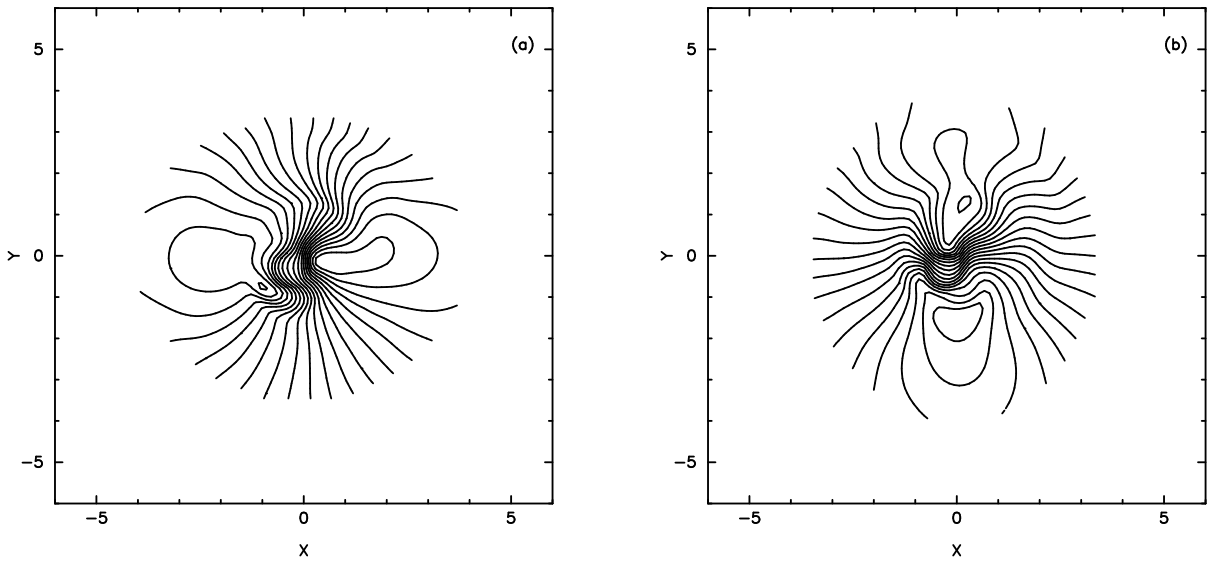

Figure 8. Two orthogonal projections of the velocity field of the disk of test particles at $t = 120$ with the disk inclined at 30° to the line of sight.

distribution becomes too patchy. Figure 8 shows the 2-D velocity field of the disk particles at time $t = 120$ "observed" from two orthogonal directions with the normal to the disk inclined at 30° to the line of sight. The extreme velocity contours close because the disk rotation curve declines at large radii. Even though the asymmetry in the mass distribution appears quite small (Figure 7), the asymmetry in the velocity field is striking.

While we do not think it likely that lop-sidedness in galaxies originates in this way, the observable consequences of lop-sidedness in any dynamical model are of some interest. Our experiment also appears to illustrate that a mild lop-sidedness in the mass distribution leads to more significant lop-sidedness in the velocity field, and may perhaps help to account for the very high incidence of asymmetries reported by Richter & Sancisi from kinematic data.

5 CONCLUSIONS

The KKDZ family of models have proved to be quite remarkably stable, except when highly flattened. As the axis ratio is increased, the lop-sided mode is the last to be stabilized in slowly rotating models, while the bar mode is the last in maximally rotating models. In the absence of extreme maximum rotation, all models with $c/a \gtrsim 0.2$ (asymptotic axis ratio 0.35) appear to be completely stable. We expect these stability properties are not specific to this mass distribution, but are characteristic of any strongly counter-streaming model (guaranteed by a 2-integral DF for a flattened mass distribution) having a uniform density core.

The addition of rotation has only a mild effect on the lop-sided mode unless all counter-streaming particles are removed. But as the net streaming motion approaches its maximum, the bar instability sets in. The sequence of maximally rotating models is again stabilized by increasing thickness, but not until $c/a \gtrsim 0.5$ (asymptotic axis ratio 0.67), although less than maximally rotating models are much more easily stabilized. We have confirmed Kalnajs's (1977) warning that the bar instability is strongly sensitive to a discontinuity in the DF across $J_z = 0$; smoothing this discontinuity in a reasonable manner reduces the net angular momentum by only a percent or two, but more than halves the growth rate of the bar.

We do not confirm the bar-forming instabilities reported by Allen *et al.* (1992) in nearly round models with net rotation, which we have shown were a numerical artifact of their code. We have

also shown that the counter-rotating bars reported by LDS and by SM probably did not result from linear instabilities, but were caused by non-linear trapping of particles in large-amplitude disturbances seeded by particle noise.

The somewhat surprising stability of the slowly-rotating models seems to be largely due to strong counter rotation. The two principal instabilities driven by counter-rotating streams of particles, the lop-sided and bending modes, are quite quickly stabilized by radial and vertical pressure respectively. We expect more realistic models that are supported by a slightly larger degree of radial pressure to be more unstable to disruptive axisymmetric bending instabilities, as found by SM, while radial motions strong enough to make the velocity ellipse radially biased would probably destabilize the radial orbit mode. We have chosen not to extend the present study to include such models, which could be created using the 3-integral DFs discussed by Dejonghe & de Zeeuw (1988), because it would be more interesting to turn to models that bear a closer resemblance to elliptical galaxies.

We would like to thank David Merritt for suggesting we undertake this study and for the use of his adaptive Kernel algorithm for preparing Figure 8. Thanks are also due to the referee, David Earn, for a careful read of the paper. This work was supported by NSF grant AST 93/18617 and NASA Theory grant NAG 5-2803.

References

Allen A. J., Palmer P., Papaloizou J., 1992, *Mon. Not. R. astr. Soc.,* **256**, 695
Antonov V. A., 1960, *Astr. Zh.*, **37**, 918 (English translation: *Soviet Astr.* **4**, 859)
Antonov V. A., 1972, in Omarov, T. B., ed, *The Dynamics of Galaxies and Star Clusters* (Alma Ata: Nauka of Kazakh SSR). English translation in de Zeeuw P. T., ed, IAU Symposium **127**, *Structure and Dynamics of Elliptical Galaxies* (1987), Reidel, Dordrecht, p. 549
Araki S., 1987, *Astr. J.,* , **94**, 99
Athanassoula E., Sellwood J. A., 1986, *Mon. Not. R. astr. Soc.,* **221**, 213
Baldwin J. E., Lynden-Bell D., Sancisi R., 1980, *Mon. Not. R. astr. Soc.,* **193**, 313
Binney J., Tremaine S., 1987, *Galactic Dynamics*, Princeton University Press, Princeton
Bishop J. L., 1987, *Astrophys. J.,* **322**, 618
Dehnen W., 1996, preprint
Dejonghe J., de Zeeuw P. T., 1988 *Astrophys. J.,* **333**, 90
de Zeeuw P. T., Franx, M., Meys, J., Brink, K., Habing, H., 1983, in Athanassoula, E., ed, IAU Symposium **100**, *Internal Kinematics and Dynamics of Galaxies*, Reidel, Dordrecht, p. 285
Earn D. J. D., 1993, *PhD thesis,* Cambridge University
Earn D. J. D., Sellwood J. A., 1995, *Astrophys. J.,* **451**, 533
Fridman A. M., Polyachenko V. L., 1984, *Physics of Gravitating Systems*, Springer-Verlag, New York
Goodman J., 1988, *Astrophys. J.,* **329**, 612
Hénon M., 1959, *Ann. d'Astrophys*, **22**, 126
Hunter, C., de Zeeuw, P. T., Park, Ch., Schwarzschild, M., 1990, *Astrophys. J.,* **363**, 367
Kalnajs A. J., 1971, *Astrophys. J.,* **166**, 275
Kalnajs A. J., 1976, *Astrophys. J.,* **205**, 751
Kalnajs A. J., 1977, *Astrophys. J.,* **212**, 637
Kuijken K., Fisher D., Merrifield M. R., 1996 (preprint – astro-ph/9606099)
Kuz'min G. G., 1956, *Astr. Zh.*, **33**, 27
Kuz'min G. G., Kutuzov S. A., 1962, *Bull Abastumani Ap Obs*, **14**, 52
Levison H. F., Richstone D. O., 1987, *Astrophys. J.,* **314**, 476
Levison H. F., Duncan M. J., Smith B. F., 1990, *Astrophys. J.,* **363**, 66 (LDS)
Lovelace R. E. V., Jore K. P., Haynes M. P., 1996, (preprint – astro-ph/9605076)
Lynden-Bell D., 1962, *Mon. Not. R. astr. Soc.,* **124**, 1

Lynden-Bell D., 1967, in Ehlers J., ed, *Relativity Theory and Astrophysics 2. Galactic Structure*, American Mathematical Society, Providence RI, p. 131
Lynden-Bell D., 1979, *Mon. Not. R. astr. Soc.,* **187**, 101
May A., Binney J., 1986, *Mon. Not. R. astr. Soc.,* **221**, 13p
Merritt D., 1987, in de Zeeuw T., ed, IAU Symposium **127**, *Structure and Dynamics of Elliptical Galaxies*, Reidel, Dordrecht, p. 315
Merritt D., Fridman T., 1996, *Astrophys. J.,* **460**, 136
Merritt D., Hernquist L., 1991, *Astrophys. J.,* **376**, 439
Merritt D., Sellwood J. A., 1994, *Astrophys. J.,* **425**, 55
Merritt D., Stiavelli M., 1990, *Astrophys. J.,* **358**, 399
Olling, R.P., 1996, *Astr. J.,* **112**, 481
Ostriker J. P., Peebles P. J. E., 1973, *Astrophys. J.,* 186, 467
Palmer P. L., 1994, *Stability of Collisionless Stellar Systems*, Kluwer, Dordrecht
Palmer P. L., Papaloizou J., Allen A. J., 1990, *Mon. Not. R. astr. Soc.,* **243**, 282
Pfenniger D., Friedli D., 1993, *Astr. Astrophys.,* **270**, 561
Qian E. E., de Zeeuw P. T., van der Marel R. P., Hunter C., 1996, *Mon. Not. R. astr. Soc.,* **274**, 602
Raha N., Sellwood J. A., James R. A., Kahn F. D., 1991, *Nature* **352**, 411
Richter O-G., Sancisi R., 1994, *Astr. Astrophys.,* , **290**, L9
Rix H-W., Zaritsky D., 1995, *Astrophys. J.,* **447**, 82
Robijn F. H. A., 1995, *PhD thesis,* Leiden University
Sackett P. D., Sparke L. S, 1990, **361**, 408
Sackett P. D., Morrison H. L., Harding P., Boroson T. A., 1994, *Nature* , **370**, 441
Saha P., 1992, *Mon. Not. R. astr. Soc.,* **254**, 132
Sellwood J. A., 1981, *Astr. Astrophys.,* **99**, 362
Sellwood J. A., 1983, *J. Comp. Phys.* **50**, 337
Sellwood J. A., 1985, *Mon. Not. R. astr. Soc.,* **217**, 127
Sellwood J. A., 1994, in Franco J., et al., eds, *Numerical Simulations in Astrophysics*, Cambridge University Press, Cambridge p. 90
Sellwood J. A., Athanassoula E., 1986, *Mon. Not. R. astr. Soc.,* **221**, 195
Sellwood J. A., Merritt D., 1994, *Astrophys. J.,* **425**, 530 (SM)
Toomre A., 1963, *Astrophys. J.,* **138**, 385
Toomre A., 1964, *Astrophys. J.,* **139**, 1217
Toomre A., 1966, in *Geophysical Fluid Dynamics*, notes on the 1966 Summer Study Program at the Woods Hole Oceanographic Institution, ref. no. 66-46, p. 111
Toomre A., 1981, in Fall S. M., Lynden-Bell D., *Structure and Evolution of Normal Galaxies*, Cambridge University Press, Cambridge, p. 111
Vandervoort P. O., 1991, *Astrophys. J.,* **377**, 49
Weinberg, M. D., 1994, *Astrophys. J.,* **420**, 597
Zang T. A., 1976 *PhD thesis,* Massachusetts Institute of Technology
Zang T. A., Hohl F., 1978, *Astrophys. J.,* **226**, 521